promoting access to White Rose research papers

Universities of Leeds, Sheffield and York
http://eprints.whiterose.ac.uk/

This is an author produced version of a paper published in ***Mechanical Systems and Signal Processing,***

White Rose Research Online URL for this paper:
http://eprints.whiterose.ac.uk/9208/

Published paper

Peng, Z.K., Jackson, M.R., Rongong, J.A., Chu, F.L. and Parkin, R.M. On the energy leakage of discrete wavelet transform. *Mechanical Systems and Signal Processing*, 2009, **23**(2), 330-343.

http://dx.doi.org/10.1016/j.ymssp.2008.05.014

White Rose Research Online
eprints@whiterose.ac.uk

On the Energy Leakage of Discrete Wavelet Transform

Z. K. Peng[1,2], M. R. Jackson[1], J. A. Rongong[3], F. L. Chu[2], R. M. Parkin[1]

[1] Mechatronics Research Group, Wolfson School of Mechanical and Manufacture Engineering, Loughborough University, Leicestershire, LE11 3UT, UK
[2] Department of Precision Instruments, Tsinghua University, Beijing 100084, P. R. China
[3] Department of Mechanical Engineering, University of Sheffield, Mappin Street, Sheffield, S1 3JD, UK

Email: pengzhike@tsinghua.org.cn; M.R.Jackson@lboro.ac.uk; J.A.Rongong@sheffield.ac.uk; chufl@mail.tsinghua.edu.cn; R.M.Parkin@lboro.ac.uk

Abstract: The energy leakage is an inherent deficiency of Discrete Wavelet Transform (DWT) which is often ignored by researchers and practitioners. In this paper, a systematic investigation into the energy leakage is reported. The DWT is briefly introduced first, and then the energy leakage phenomenon is described using a numerical example as an illustration and its effect on the DWT results is discussed. Focusing on the *Daubechies* wavelet functions, the band overlap between the quadrature mirror analysis filters was studied and the results reveal that there is an unavoidable tradeoff between the band overlap degree and the time resolution for the DWT. The dependency of the energy leakage to the wavelet function order was studied by using a criterion defined to evaluate the severity of the energy leakage. In addition, a method based on resampling technique was proposed to relieve the effects of the energy leakage. The effectiveness of the proposed method has been validated by numerical simulation study and experimental study.

1 Introduction

The last 20 years have seen remarkable progresses in both theoretical studies and application developments of Wavelet transform (WT) [1]. The great popularity of the WT among the researchers has been indicated by the numerous literatures from various academic research communities [2]~[8]. The research activities related to the WT are so broadly that a comprehensive review on it is certainly impossible. While people are praising the powerful capacities of the WT, enjoying the benefits from the WT and being encouraged for the achievements provided by the WT, few attentions have been paid to the inherent deficiencies of the WT such as the border distortion [9] and the energy leakage [10][11]. The border distortion is also known as boundary effect which is usually caused by the insufficient data points both at the beginning and at the end of finite-duration signals and can usually be alleviated to certain extent by implementing the zero-padding or symmetric extending to the signals. Compared to the border distortion, the energy leakage has received much less attentions. Only a few researchers [10][11] have noticed this deficiency but have only made very brief mention to it, and no further investigation has been carried out on this issue. However, as will be revealed in this paper, the energy leakage can make significant effects to the outputs of the Discrete Wavelet Transforms (DWTs). Understanding the effects of the energy leakage to the DWT outputs and the dependency of the energy leakage to the wavelet functions is therefore of great benefit in helping people to select appropriate wavelet function to meet their specific demands.

This paper will be devoted to systematic investigations of the energy leakage for DWTs. Rather than insisting on mathematical deductions this study will focus on the example illustrations which are often more intelligible. In Section 2, the DWT method will be briefly introduced first, and energy leakage phenomenon is then illustrated using a numerical example and its effects on the DWT outputs will be discussed. Second, the dependency of the energy leakage to the wavelet functions will then be discussed and a criterion will be defined to evaluate the severity of the energy leakage. In Section 3, a simple method based on resampling technique is put forward to relieve the effects of the energy leakage. The effectiveness of the proposed technique is validated by numerical simulation and experimental studies. Finally conclusions are given in Section 4.

2 Energy Leakage of Discrete Wavelet Transform

So far the WT has been well-familiar to people. There is a rich collection of literature available on the DWT and, therefore, before introducing the energy leakage of the DWT, only a brief recap on the DWT is presented.

2.1 Discrete Wavelet Transform [12]

Regarding the sampled signal $f(t)$ as a discrete approximation $A_0 f$ of resolution $2^{-(0+1)}$=1/2, then a N-level DWT can decompose the sampled signal $f(t)$ into one approximation $A_N f$ of resolution $2^{-(N+1)}$ and N details $D_j f$ of resolutions $2^{-(j+1)}$ $(1 \le j \le N)$. The practical procedure for the application of DWT is known as Mallat's algorithm. According to the Mallat's algorithm, the approximation $A_{j+1} f$ and the detail $D_{j+1} f$ can be obtained by performing the decomposition to $A_j f$, as follows.

$$A_{j+1} f = \sum_k h(k-2n) A_j f \qquad (1)$$

$$D_{j+1} f = \sum_k g(k-2n) A_j f \qquad (2)$$

where $h(n)$ is the half-band low-pass analysis filter and $g(n)$ is the half-band high-pass analysis filter. It is important that the two filters are related to each other and they are known as a quadrature mirror analysis filter. The one stage decomposition is illustrated as Fig 1. It is worth pointing out that the decomposition has halved the time resolution since only half of each filter output characterizes the signal. However, each output has half the frequency band of the input so the frequency resolution has been doubled.

[Fig 1]

According to the DWT theory, if a N-level DWT is implemented on the signal $f(t)$ of sampling frequency F_s, then ideally the details $D_j f$ $(1 \le j \le N)$ should only contain the information concerning the signal components whose frequencies are included in the interval $[2^{-(j+1)}F_s, 2^{-j}F_s]$ $(1 \le j \le N)$ and the approximation $A_N f$ should contain the information related to the low frequency component belonging to the interval $[0, 2^{-(N+1)}F_s]$. The ideal frequency domain division performed by the DWT is shown as Fig 2. However, to achieve the ideal division in frequency domain, the frequency response functions (FRFs) of the quadrature mirror analysis filters $h(n)$ and $g(n)$ are required to be of the ideal forms shown in Fig 3, which has been proved never achievable in practice because the band overlap between the quadrature mirror analysis filters $h(n)$ and $g(n)$ is always inevitable no matter whatever wavelet function is adopted, for example *DB7* whose corresponding quadrature mirror analysis filters are shown in Fig 4. It is just the band overlap between the quadrature mirror analysis filters that cause the energy leakage deficiency to the DWT.

[Fig 2]

[Fig 3]

[Fig 4]

2.2 Energy Leakage of DWT

To demonstrate the energy leakage of the DWT, consider a signal generated by function *randn* of Matlab, which is normal distribution with mean zero, variance one and standard deviation one. The spectrum of the generated random signal is shown in Fig 5. Three-level DWT is performed to the signal with wavelet function *DB8*. The spectra of the approximation A_3f and three details D_3f, D_2f and D_1f are shown in Fig 6(a), (b), (c) and (d) respectively. The frequency components in the boxes are the essential components which the corresponding approximation or details should only contain, but the frequency components out of the boxes are the components caused by the energy leakage. Clearly, the energy leakages occur between all two adjacent bands.

[Fig 5]

[Fig 6]

As an inherent deficiency of the DWT, the severity of the energy leakage is mainly determined by the specific wavelet function used to execute the DWT procedure. Usually, when a wavelet function whose corresponding quadrature mirror analysis filters $h(n)$ and $g(n)$ have big band overlap is used to conduct the DWT, then the DWT results would be of strong energy leakage, and vice versa. The frequency band overlap between the quadrature mirror analysis filters varies with the Wavelet function type, for example the band overlap for the higher order *Daubechies* wavelet function is smaller than for the lower order *Daubechies* wavelet function. Fig 7 shows the FRFs of quadrature mirror analysis filters of the wavelet functions *DB4*, *DB14*, *DB24* and *D34,* among which, apparently, *DB4* has the biggest band overlap, and *DB14* is the next, and *DB34* has the smallest band overlap. The degree of the frequency band overlap can be quantitatively measured using the index (BOI : Band Overlap Index) defined as follows

$$BOI = \frac{\int_{0}^{0.25} \left| FRF_g(j\omega) \right| d\omega}{\int_{0.25}^{0.5} \left| FRF_g(j\omega) \right| d\omega} \tag{3}$$

Where $FRF_g(j\omega)$ is the *FRF* of the half-band high-pass analysis filter $g(n)$. Fig 8 shows the *BOIs* for the wavelet functions *DB3~DB44*. It can be seen that the *BOIs* steadily decrease with the order of the *Daubechies* wavelet function.

The dependency between the *BOI* and the *Daubechies* wavelet function order indicates that in order to achieve results of low level energy leakage it has to employ higher order *Daubechies* wavelet functions to execute the DWTs. However, the higher order *Daubechies* wavelet functions will result in the resolution decrease in time domain as the high order *Daubechies* wavelet functions have longer support in time domain than the low order *Daubechies* wavelet functions. It is well known that due to the limitation defined by the Heisenberg-Gabor inequality [13][14] it is impossible for Continuous Wavelet Transform (CWT) to obtain both fine resolutions in time and in frequency at the same window defined in the time-frequency plane, and therefore the tradeoff between time and spectral resolutions is unavoidable. Interestingly, the dependency between the *BOI* and the *Daubechies* wavelet function order reveals that there is also an unavoidable tradeoff between the band overlap degree and the time resolution for the DWT.

[Fig 7]

[Fig 8]

The spectra of the approximation and details shown in Fig 6 have confirmed that the frequency band overlap between the quadrature mirror analysis filters can introduce energy leakage to the DWT results. To determine the energy leakage severities of all the approximation and details for different wavelet functions, the normal distribution signals are considered once more. As shown in Fig 5, the spectra of the normal distribution signals are also normal distribution in frequency domain and this property enable them to offer people a convenient way to estimate the energy leakage severities at different decomposition levels for different wavelet functions. From the spectra of normal distribution signals, the energy leakage severities of $A_N f$ and $D_j f$ ($1 \le j \le N$) can be estimated using the variables $ELS_{(A,N)}$ and $ELS_{(D,j)}$ respectively which are defined as follows.

$$ELS_{(A,N)} = \frac{1}{M}\sum_{k=1}^{M}\left(1-\frac{\int_0^{2^{-(N+1)}}\left|F_{(A,N,k)}(\omega)\right|d\omega}{\int_0^{2^{-1}}\left|F_{(A,N,k)}(\omega)\right|d\omega}\right) \quad (4)$$

$$ELS_{(D,j)} = \frac{1}{M}\sum_{k=1}^{M}\left(1-\frac{\int_{2^{-(j+1)}}^{2^{-j}}\left|F_{(D,j,k)}(\omega)\right|d\omega}{\int_0^{2^{-1}}\left|F_{(D,j,k)}(\omega)\right|d\omega}\right) \quad (1 \le j \le N) \ (5)$$

Where $F_{(A,N,k)}(\omega)$ and $F_{(D,j,k)}(\omega)$ are the spectra of $A_N f$ and $D_j f$ ($1 \le j \le N$), and M is the number of the normal distribution signals which have been used to estimate the energy leakage severity. The $ELS_{(A,N)}$ and $ELS_{(D,j)}$ with M = 200 have been used to estimate the energy leakage severities of $A_5 f$ and $D_j f$ ($1 \le j \le 5$) for *Daubechies* wavelet functions *DB3~DB44*, and the results are shown in Fig 9.

[Fig 9]

The results shown in Fig 9 clearly indicate that the high order details always have worse energy leakages than the low order details, and the energy leakage of $D_1 f$ is relatively low compared to the others. In addition, it can be seen from Fig 9 that the energy leakage severities sharply decrease with the increase of the wavelet function order between order 3 to order 20. However, between order 20 to order 44, increasing the wavelet function order can only slightly improve the energy leakage. This indicates that to reach an optimal balance between the energy leakage and the time resolution it is better to use *Daubechies* wavelet functions around order 20 to perform the DWT.

2.3 Discussions on Effects of the Energy Leakage

Since the advent of the wavelet transform method, it has been widely used in many research activities. Apart from the original intention of the wavelet transform for the analysis of non-stationary signals [15][16], other important and successful applications of the wavelet transform include the denoising study [7][17][18], data compression [19][20] and the feature extraction [21][22] *et al*. The successes in the latter three applications have mainly benefited from an important property of the WT: the basis wavelet functions used in the wavelet transforms are often of compact support and so wavelet transforms have good energy concentration and, therefore, most coefficients are usually very small, and can be discarded without causing significant errors for signal representations. Therefore, the wavelet transform can represent the signal with a limited number of coefficients. In addition, if the signal is contaminated by noise, the energy of the noise component of the signal will usually be dispersed throughout the transform as relatively small coefficients. This gives options to use simple methods to eliminate the noise. In many feature extraction studies, the few significant coefficients have been directly used as the features or, based on which some other kinds of features have been suggested, i.e. the wavelet energy based feature. The signal compression principles are also similar to the denoising, that is, only keeping the few significant coefficients and setting the other small coefficients to zero so that it is able to use a few bits to represent the signal during encoding. In all the three applications, the coefficients with big amplitudes will play more important roles than the coefficients with small amplitudes. However, due to the deficiency of the energy leakage, it is very likely that the frequency components around the dyadic frequencies, i.e. $2^{-(j+1)}F_s$ $(1 \le j \le N)$ will be split into two adjacent bands and, consequently, the amplitudes of the associated coefficients are reduced, for example the components around frequency $2^{-2}F_s$ would be split into $D_1 f$ and $D_2 f$. In addition, as discussed in Section 2.2, how much energy will be leaked is also dependent on the used wavelet functions, and the lower order wavelet functions can cause more energy leakage. To demonstrate this, a signal consisting of four frequency components is considered, as follows

$$f(t) = \begin{cases} \sin(380\pi t) & 0 \le t \le 0.5 \\ \sin(480\pi t) & 0.5 < t \le 1 \\ \sin(520\pi t) & 1 < t \le 1.5 \\ \sin(800\pi t) & 1.5 < t \le 2 \end{cases} \tag{6}$$

The signal was sampled with a sampling rate of 1000Hz. According to the wavelet theory, if the 2-level DWT is conducted on the signal, ideally the components with frequencies 260Hz and 400Hz would appear only in $D_1 f$ and their associated coefficients should be of the same amplitudes. Similarly, the components with frequencies 190Hz and 240Hz would appear only in D_2f and their associated coefficients should be of the same amplitudes. Moreover, the coefficients of A_2f would be very close to zero as there is no frequency component in the signal locating at the frequency band of A_2f.

[Fig 10]
[Fig 11]

Figs 10 and 11 show the results obtained by using wavelet functions *DB10* and *DB40* respectively. It can be seen from both Fig 10 and Fig 11 that considerable energy of the 260Hz component has been leaked from D_1f to D_2f and its corresponding coefficients are smaller than the coefficients of the 400Hz component. The same situation has also happened to the 240Hz component, part of whose energy has been leaked from D_2f to D_1f and whose associated coefficients are smaller than the coefficients related to the 190Hz component. The results imply that the components close to the dyadic frequencies will suffer more energy leakage than the components away from the dyadic frequencies. In addition, the results also indicate that both the coefficients associated to the 240Hz component in D_1f and the coefficients associated to the 260Hz component in D_2f are of bigger amplitudes at Fig 10 than at Fig 11. Moreover, it can be found that in Fig 10 little energy of the 190Hz component has been leaked to D_1f, however there was no energy leakage with this component in Fig 11. All these confirm that the energy leakage can cause amplitude decrease to the affected coefficients and *DB10* can lead to worse energy leakage than *DB40*. Note that the nonzero coefficients at the two ends of A_2f are just the so called border distortion.

3 An Anti-Energy-Leakage Method for DWT

3.1 The Anti-Energy-Leakage Method

Above analysis has clearly indicated that, as an inherent deficiency, the energy leakage is inevitable for the DWT, and the severity of the leakage is to certain degree dependent on the wavelet function type used to execute the transform. Therefore, to relieve the effects of the energy leakage on the wavelet transform results, it is better to select wavelet functions with as high orders as possible under the condition the desired time resolution can be guaranteed. Moreover, above analysis has also shown that the frequency components close to the dyadic frequencies will suffer more energy leakage than the frequency component far from the dyadic frequencies. This means that it is possible to relieve the effects of the energy leakage by shifting the frequency components from the positions close to the dyadic frequencies to the positions away from the dyadic frequencies, which can be reached simply by using a resampling method. For example, for a signal containing a 250Hz frequency component, if the initial sampling frequency is 1000Hz, then severe energy leakage could happen to the 250Hz component when conducting DWT on the signal. However, if a resampling procedure is applied to the signal with a sampling rate of 1300Hz before the DWT, then the energy leakage to the 250Hz component can be relieved to a certain degree.

Usually, real signals are often very complicated and contain more than one frequency components and, therefore, it is impossible to avoid the energy leakage for all frequency components by changing the sampling frequency. In this situation, the resampling rate can be selected to the one which can relieve the energy leakage for the frequency components of particular interests. In case the information loss during resampling, up-sampling should be considered. After introducing the resampling procedure, the one stage decomposition of the DWT can be modified as follows:

1, *Resampling Procedure* (*F_j is the sampling frequency of $A_j f$*)
    If there are frequency components of interest close to the $2^{-2}F_j$
        Resampling $A_j f$ with a new sampling frequency $F_{j(\mathrm{new})}$.
    Else
        Without resampling $F_{j(\mathrm{new})} = F_j$.
2, *Decomposition*
    Carry out the standard DWT decomposition to the new $A_j f$ after resampling

This anti-energy-leakage decomposition can also be illustrated as

[Fig 12]

Accordingly, the reconstruction operation in the inverse DWT should be modified as

[Fig 13]

Here $\underline{h}(n)$ and $\underline{g}(n)$ are the quadrature mirror synthesis filters.

Actually, by introducing the resampling procedure before the one-stage decomposition, it can reach an arbitrary division in the frequency domain rather than only the strictly dyadic division shown in Fig 2.

3.2 Numerical and Experimental Validations

Case 1: Numerical Validation

To validate the effectiveness of the resampling procedure in relieving the energy leakage, below linear chirp signal is considered

$$f(t) = 0.5\sin(2\pi(40t + t^2)) \qquad (0 \le t \le 10) \quad (7)$$

A strong white noise whose maximal amplitude is equal to 0.5 has been artificially added to the chirp signal. Initially the signal has been sampled using the sampling rate of 400Hz. To remove the noise from the signal, the 5-level DWT has been carried out using *DB20* on the noise chirp signal and the hard threshold is set to 0.5.

In this case, the only interesting component is the chirp component whose frequency range is from 40Hz to 60Hz. Obviously, the frequency range of the chirp component will cover the dyadic frequency 50Hz between D_2f and D_3f when the sampling frequency F_s is 400Hz, and so the energy leakage could happen to the chirp component. Fig 14 shows the wavelet transform results for the case of F_s = 400 Hz. It can be seen that the energy of the chirp component has been split into D_2f and D_3f. After applying the resampling procedure with new sampling frequency of 600Hz to the original signal, the wavelet transform results then became what shown in Fig 15. Clearly, most energy of the chirp component has concentrated at D_3f. In denoising, all coefficients whose absolute values are smaller than the hard threshold 0.5 are set to zero, and the inverse DWT is conducted on the remaining coefficients. Fig 16 and Fig 17 show the spectra of the chirp signal after denoising with and without resampling procedure. Apparently, the method with resampling procedure has performed better in denoising than the method without resampling procedure. More noise component between 50~100Hz has been suppressed in Fig 17 than in Fig 16. This numerical study has validated the effectiveness of the resampling procedure in relieving the energy leakage.

[Fig 14]
[Fig 15]
[Fig 16]
[Fig 17]

Case 2: Experimental Validation

To further verify the effectiveness of the anti-energy-leakage method, an experimental data, which was sampled from a real rotor system with coupling misalignment fault, is inspected. The real rotor system is shown in Fig 18, and more details about which can be found in Ref [23].

[Fig 18]

The experimental vibration signal was collected using non-contact eddy-current transducers at a sampling rate of 1.6 kHz. The rotational speed of the rotor system was set at 3000 rpm. To well demonstrate the proposed method, a strong white noise was artificially imposed on the sampled vibration signal, and the strength of the noise component is half of the sampled signal in amplitude. The temporal waveform of the signal contaminated by noise is shown in Fig 19 (a) together with its FFT spectrum in

Fig 19(b).

[Fig 19]

Obviously, from Fig 19(b) it can be seen that, besides the fundamental harmonic component 1X, the other significant frequency component is the second harmonic 2X. The increasing of the second harmonic 2X is the main frequency feature of the coupling misalignment fault for rotor machines. When applying denoising procedure on this vibration signal, it is better to keep the energy of the 2X component as much as possible. However, it is easy to find that the frequency of the 2X component is 100 Hz and is 1/16 of the sampling frequency. According to the frequency domain division of DWT, when the standard DWT denoising method with 3-level decomposition is applied to this vibration signal, the energy of the 2X component would be separated into D3 and A3. That is just the undesired situation discussed in last section. To avoid the energy leakage on the 2X component, it is necessary to resample the vibration signal with different sampling frequency before carrying out the denoising procedure. The routine *wden* in the commercial software Matlab 7.0 is used with *DB20* wavelet function and 3-level decomposition to execute the denoising task. Fig 20 and Fig 21 show the spectra of the coupling misalignment vibration signal after denoising with and without resampling. The resampling rate is 1.9 kHz. It can been seen from Fig 20 that the second harmonic 2X after denoising is smaller than that before denoising due to the energy leakage. On the contrary, the resampling procedure has successfully prevented the 2X component from the energy leakage as indicated by Fig 21. For a better comparison, the moduli of the 2X components before denoising and after two different denoising are list in Table 1. Obviously, the resampling procedure has considerably relieved the energy leakage to the 2X component. This experimental study has further validated the effectiveness of the resampling procedure in relieving the energy leakage.

[Fig 20]

[Fig 21]

Table 1, the modulus of 2X before and after denoising

	Without Denoising	After the Standard Denoising	After the Improved Denoising
Modulus of 2X	3.1184	2.2827	2.9656

4 Conclusions

In this paper, an inherent deficiency of the Discrete Wavelet Transform - energy leakage has been investigated. The results have shown that it is the frequency band overlap between the quadrature mirror analysis filters that leads to the energy leakage for the DWT. Moreover, the frequency band overlap is inevitable and there is a tradeoff between the band overlap degree and the time resolution for the DWT as the lower order wavelet functions will suffer bigger frequency band overlap than the higher order wavelet functions and *vice versa*. The relationship between the band overlap and the wavelet function order has also determined the dependency of the energy leakage to the wavelet function order. The studies have revealed that, to relieve the effects of the energy leakage on the wavelet transform results, it is better to select wavelet functions with as high orders as possible under the condition the desired time resolution can be guaranteed. In addition, the studies have also shown that the frequency components close to the dyadic frequencies will suffer more energy leakage than the frequency component far from the dyadic frequencies. Starting from the observation, a method based on resampling technique has been proposed to relieve the effects of the energy leakage. The effectiveness of the proposed method has been validated by numerical simulation study and experimental study. It is worth noting that no method can eliminate the energy leakage completely for the DWT, and the proposed method in this study can only to a certain degree relieve the effects of energy leakage for the selected frequency components of particular interests.

Acknowledgements

The authors gratefully acknowledge the supports of EPSRC founder IMCRC at Loughborough University (IMRC198), UK, and the Natural Science Foundation of China (No.50425516), for this work.

References

1. Z. K. Peng, F. L. Chu, Application of the wavelet transform in machine condition monitoring and fault diagnostics: a review with bibliography, *Mechanical Systems and Signal Processing*, **18 (**2004) 199-221
2. F. Argoul, A. Arnéodo and *et al*, Wavelet analysis of turbulence reveals the multifractal nature of the Richardson cascade, *Nature*, **338** (1989), 51- 53
3. PC Ivanov, MG Rosenblum and et al, Scaling behavior of heartbeat intervals obtained by wavelet-based time series analysis, *Nature*, **383** (1996) 323-327
4. K. M. Lau, H.Y Weng, Climate signal detection using wavelet transform: how to make a time series sing, *Bulletin of the American Meteorological Society,* **76** (1995) 2391-2402
5. P Abry P, D. Veitch, Wavelet analysis of long-range-dependent traffic, *IEEE*

Transactions on Information Theory, **44** (1998) 2-15

6. M Antonini, M Barlaud, P Mathieu, I Daubechies, Image coding using wavelet transform, *IEEE Transactions on Image Processing*, **1** (1992) 205-220
7. L Sendur, I.W. Selesnick, Bivariate shrinkage functions for wavelet-based denoising exploiting interscale dependency, *IEEE Transactions on Signal Processing*, **50** (2002) 2744- 2756
8. W. G. Zanardelli, E. G. Strangasa, H.K. Khalila, J. M. Miller, Wavelet-based methods for the prognosis of mechanical and electrical failures in electric motors, *Mechanical Systems and Signal Processing*, **19** (2005) 411-426
9. C Taswell, K. C. McGill, Wavelet transform algorithms for finite-duration discrete-time signals. *ACM Trans. Math. Software*, **20** (1994), 398-412.
10. J Qiu, U Paw , T Kyaw, R.H. Shaw, The leakage problem of orthonormal wavelet transforms when applied to atmospheric turbulence, *Journal of Geophysical Research*, **100** (1995) 25769-25780
11. J. Antonino-Daviu, P. Jover, M. Riera and *et al*, DWT analysis of numerical and experimental data for the diagnosis of dynamic eccentricities in induction motors, *Mechanical Systems and Signal Processing* **21** (2007) 2575-2589
12. S. G. Mallat. *A Wavelet Tour of Signal Processing*, Academic Press, San Diego (1998).
13. Z. K. Peng, F. L. Chu, Peter W. Tse, Detection of the rubbing-caused impacts for rotor–stator fault diagnosis using reassigned scalogram, *Mechanical Systems and Signal Processing,* **19** (2005) 391- 409
14. F Auger, P Flandrin. Improving the readability of time-frequency and time-scale representations by the reassignment method. *IEEE Transactions on Signal Processing* **43 (**1995**)** 1068-1089
15. E. Douka, S. Loutridis, A. Trochidis, Crack identification in plates using wavelet analysis. *Journal of Sound and Vibration*, **270** (2004) 279-295
16. T Inoue, A Sueoka, H Kanemoto and *et al*, Detection of minute signs of a small fault in a periodic or a quasi-periodic signal by the harmonic wavelet transform, *Mechanical Systems and Signal Processing*, **21**(2007) 2041-2055
17. Y. Y. Kim, J. C. Hong, N. Y. Lee, Frequency response function estimation via a robust wavelet de-noising method, *Journal of Sound and Vibration*, **244** (2001) 635-649
18. C Taswell, The what, how, and why of wavelet shrinkage denoising, *Computing in Science & Engineering*, **2** (2000) 12-19

19. W.J. Staszewski, Wavelet based compression and feature selection for vibration analysis. *Journal of Sound and Vibration* **211** (1998) 735-760
20. M. Tanaka, M. Sakawa, K. Kato *et al.*, Application of wavelet transform to compression of mechanical vibration data. *Cybernetics and Systems* **28** (1997) 225-244
21. H Hong, M Liang, Separation of fault features from a single-channel mechanical signal mixture using wavelet decomposition, *Mechanical Systems and Signal Processing*, **21**(2007) 2025-2040
22. Q Hu, Z.J He, Z.S Zhang, Y.Y Zi, Fault diagnosis of rotating machinery based on improved wavelet package transform and SVMs ensemble, *Mechanical Systems and Signal Processing*, **21** (2007) 688-705
23. Z. Peng, Y. He, Z. Chen and F. Chu, Identification of the Shaft Orbit for Rotating Machines Using Wavelet Modulus Maxima. *Mechanical Systems and Signal Processing*, **16**(2002) 623-635

List of the Figure Captions

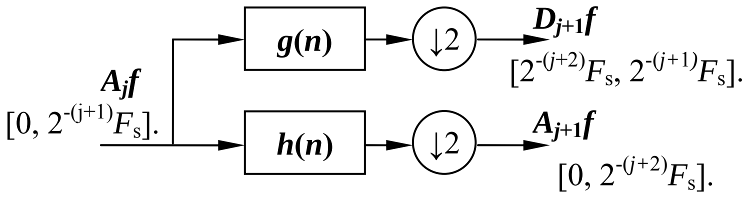

Fig 1, one stage decomposition

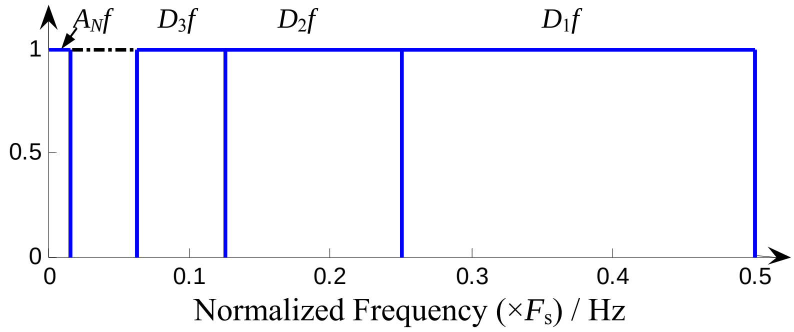

Fig 2, the ideal frequency domain division of DWT

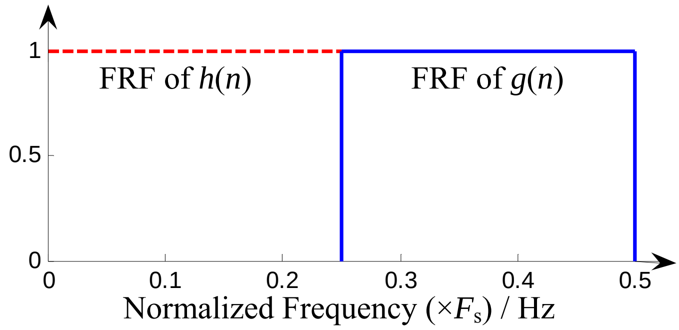

Fig 3, the ideal FRFs of the quadrature mirror analysis filters

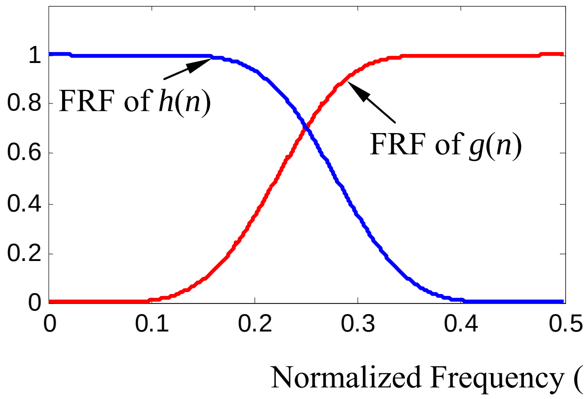

Matlab Codes

```
[Lo_D, Hi_D] = wfilters('db7');
[Hi, Fq1] = freqz(Hi_D);
[Lo, Fq2] = freqz(Lo_D);
plot(Fq1/2/pi, abs(Hi)/sqrt(2));
hold on
plot(Fq2/2/pi, abs(Lo)/sqrt(2));
set(gca, 'XLim', [0, 0.5])
```

Fig 4, the quadrature mirror analysis filters of *DB7*

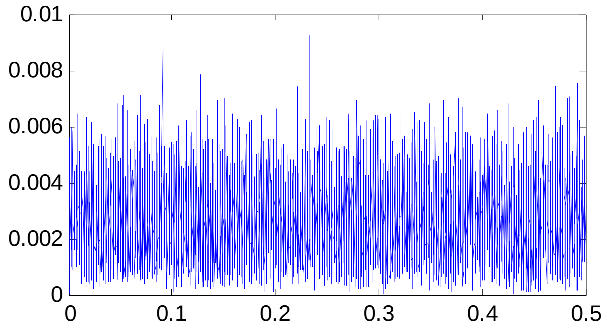

Fig 5, the FFT spectrum of the random signal

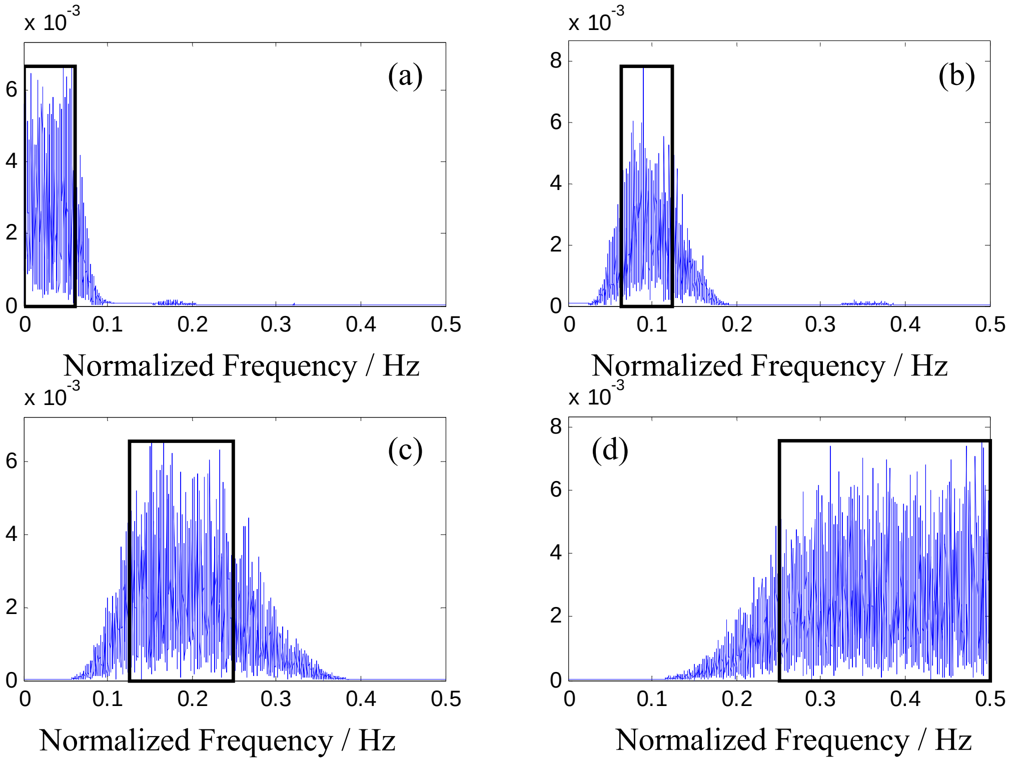

Fig 6, the FFT spectra of the approximation and three details

[(a) A_3f ; (b) D_3f; (c) D_2f; (d) D_1f]

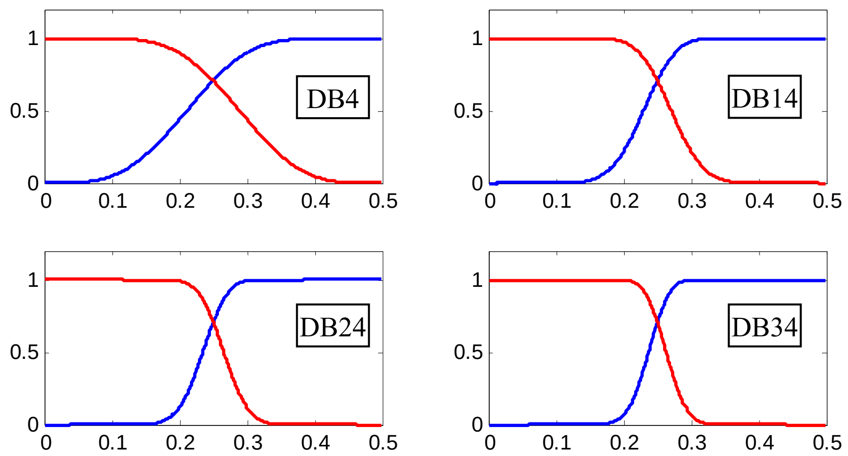

Normalized Frequency / Hz

Fig 7, the quadrature mirror analysis filters of *DB4*, *DB14*, *DB24* and *D34*

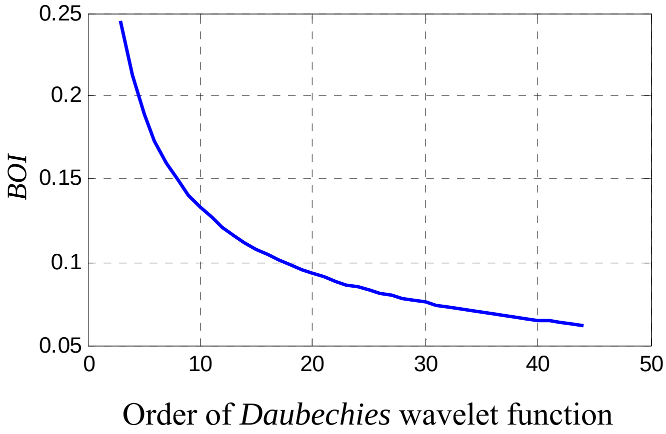

Fig 8, *BOI*s of *Daubechies* wavelet functions

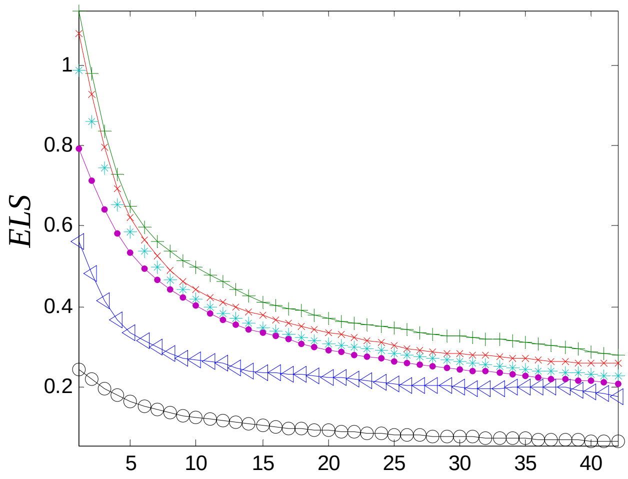

Fig 9, The relationship between energy leakage severities and wavelet function order. [Δ - A_5f; + - D_5f; × - D_4f; ∗ - D_3f; · - D_2f; o - D_1f]

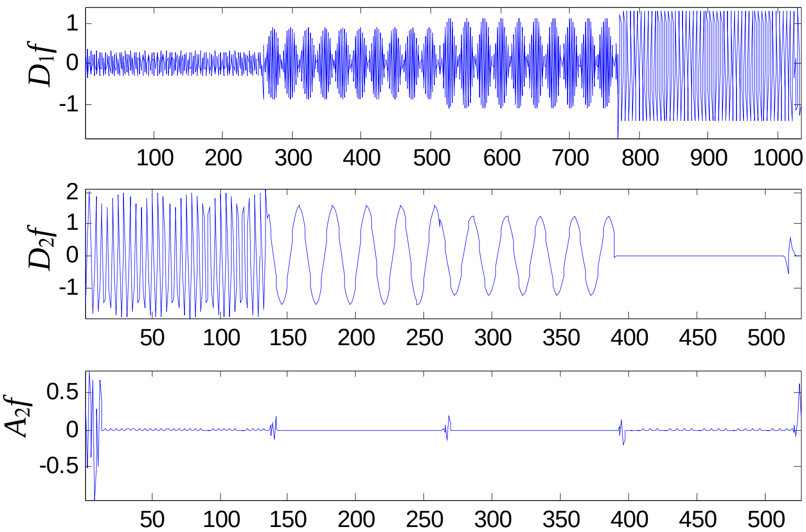

Fig 10, the wavelet transform results by *DB10*

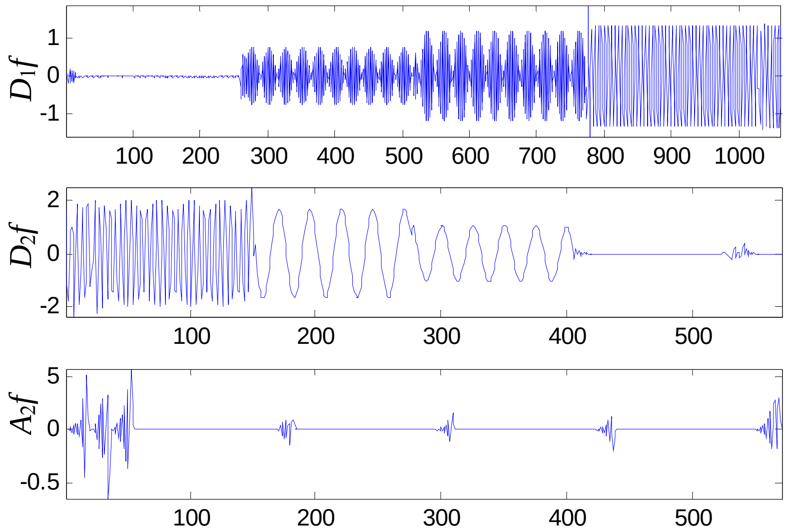

Fig 11, the wavelet transform results by *DB40*

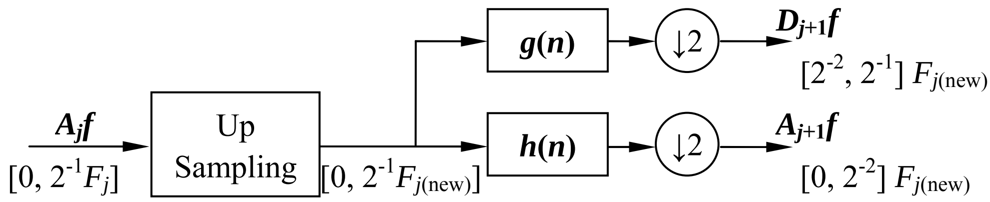

Fig 12, the anti-energy-leakage decomposition

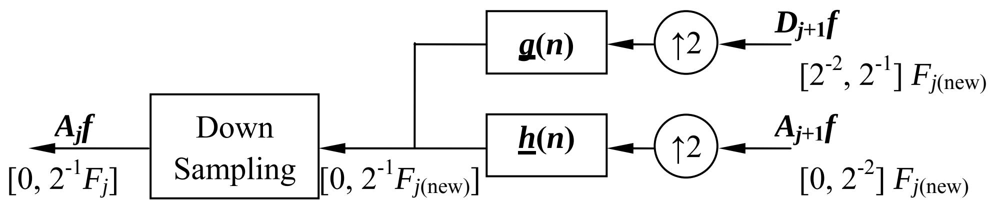

Fig 13, the anti-energy-leakage reconstruction

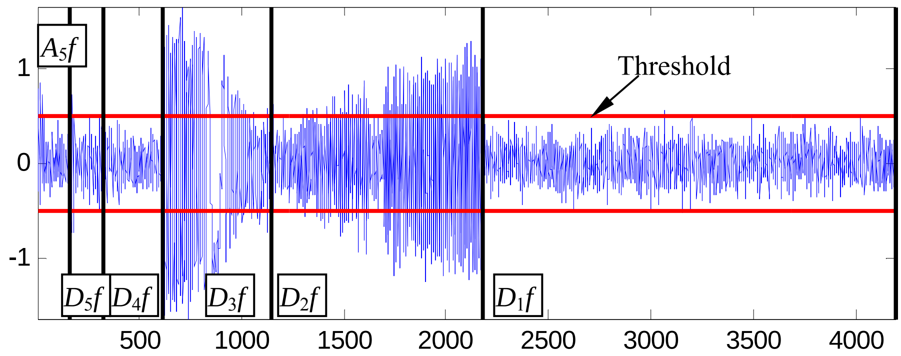

Fig 14, the wavelet transform coefficients [F_s = 400Hz]

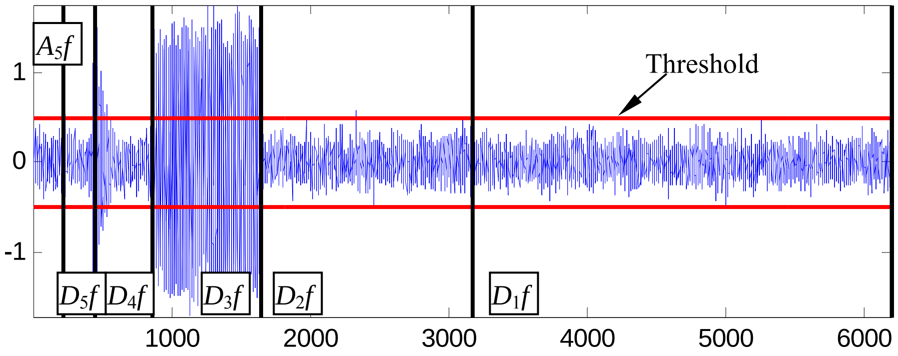

Fig 15, the wavelet transform coefficients [F_s = 600Hz]

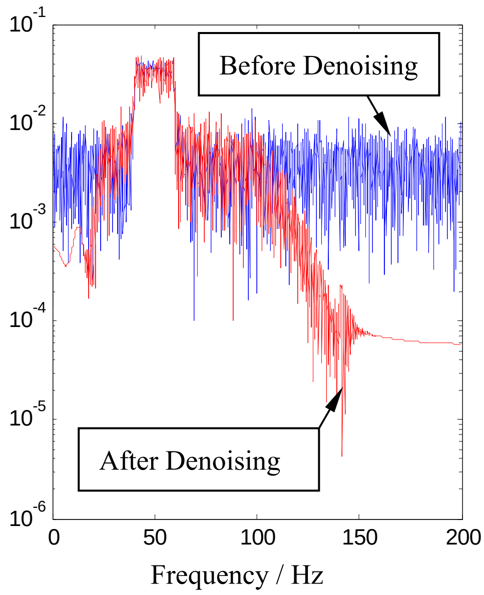

Fig 16, The spectra of the signal before denoising and after denoising without resampling procedure

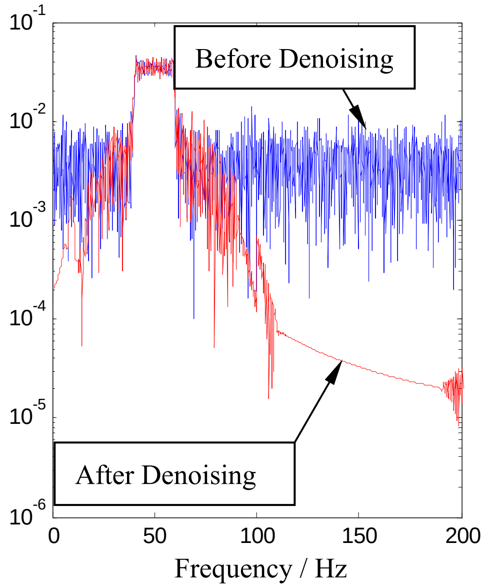

Fig 17, The spectra of the signal before denoising and after denoising with resampling procedure

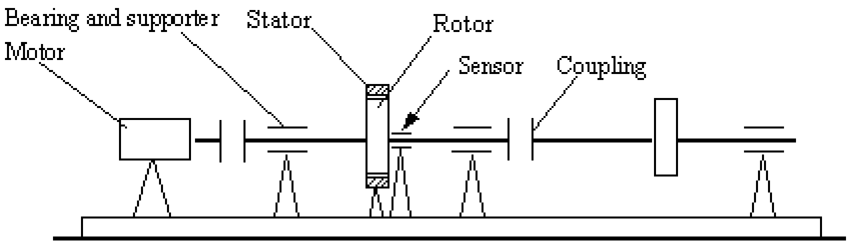

Fig. 18. Experimental test rig of a real rotor system.

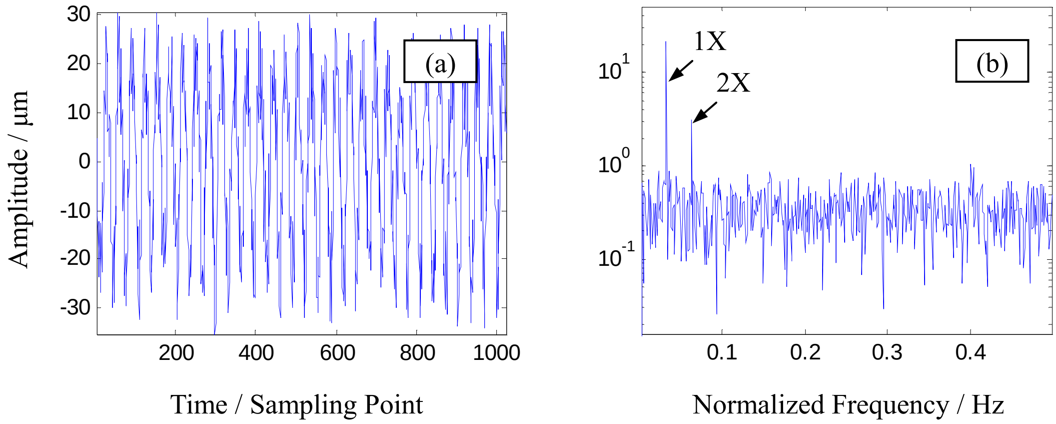

Fig 19, (a) The temporal waveform of the coupling misalignment fault signal and (b) its FFT spectrum

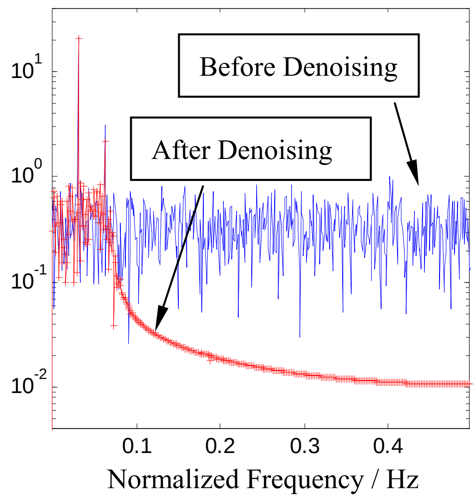

Fig 20, The spectra of the coupling misalignment signal before denoising and after denoising without resampling procedure

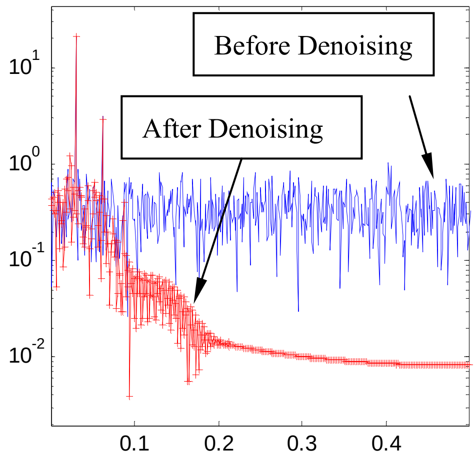

Fig 21, The spectra of the coupling misalignment signal before denoising and after denoising with resampling procedure